Supporting Information

Oxygen-redox activity in non-Li-excess W-doped $LiNiO_2$ cathode

A. S. Menon[1,2,§] B. J. Johnston,[2,3,§] S. G. Booth,[2,3,4] L. Zhang,[2,5] K. Kress,[2,3] B. Murdock,[5] G. Paez Fajardo,[1,2] N. N. Anthonisamy[2,3,8] N. Tapia-Ruiz,[2,5,6] S. Agrestini,[7] M. Garcia-Fernandez,[7] K. Zhou,[7] P. K. Thakur,[7] T. L. Lee,[7] A. J. Nedoma,[2,9] S. A. Cussen[2,3,*] and L. F. J. Piper[1,2,*]

[1] *WMG, University of Warwick, Coventry CV4 7AL, UK*
[2] *The Faraday Institution, Quad One, Harwell Campus, Didcot OX11 0RA, UK*
[3] *Department of Materials Science and Engineering, The University of Sheffield, Sheffield S1 3JD, UK*
[4] *Integrated Graphene Ltd. Euro House, Stirling FK8 2DJ, UK*
[5] *Department of Chemistry, Lancaster University, Lancaster LA1 4YB, UK*
[6] *Department of Chemistry, Molecular Sciences Research Hub, White City Campus, Imperial College London, London W12 0BZ, UK*
[7] *Diamond Light Source Ltd., Diamond House, Harwell Science and Innovation Campus, Didcot OX11 0DE, UK*
[8] *Jaguar Land Rover Inc., Coventry CV3 4LF, UK*
[9] *Department of Chemical and Biological Engineering, University of Sheffield, Sheffield S1 3JD, UK*

[§]These authors contributed equally to this work.
*Corresponding authors email addresses: Louis.Piper@Warwick.ac.uk and S.Cussen@Sheffield.ac.uk

Contents

1. XRD analysis of pristine WLNO

1.1 $R\bar{3}m$ unit cell refinement

Pawley refinement[1] was performed to obtain the rhombohedral ($R\bar{3}m$) unit cell parameters of WLNO. The starting parameters were obtained from Ref.[10]. The emission profile was calculated using data collected from a Si standard. For the unit cell refinements, a modified Thompson-Cox-Hastings pseudo-Voigt peak shape function (*TCHZ_Peak_Type*) together with a function for the peak asymmetry (*Simple_Axial_Model*) was used to model the peak shapes. The *Simple_Axial_Model*, which is an instrument-related parameter, was also allowed to refine due to the presence of the Bragg reflections at angles lower than that contained in the data from the standard sample. A 6th degree Chebyshev polynomial was used to fit the background. The peak shape functions are defined in the TOPAS Academic technical reference manual available online.

Table S1: Refined lattice parameters of a rhombohedral ($R\bar{3}m$) unit cell. R_{wp} and GoF denote the R-weighted pattern and goodness of fit, respectively, and are defined in the TOPAS Academic technical reference manual.

R_{wp}	GoF	a (Å)	c (Å)	Vol. (Å^3)
5.82	3.6	2.88369(1)	14.2067(7)	102.311(7)

1.2 Comparison of WLNO and undoped $LiNiO_2$

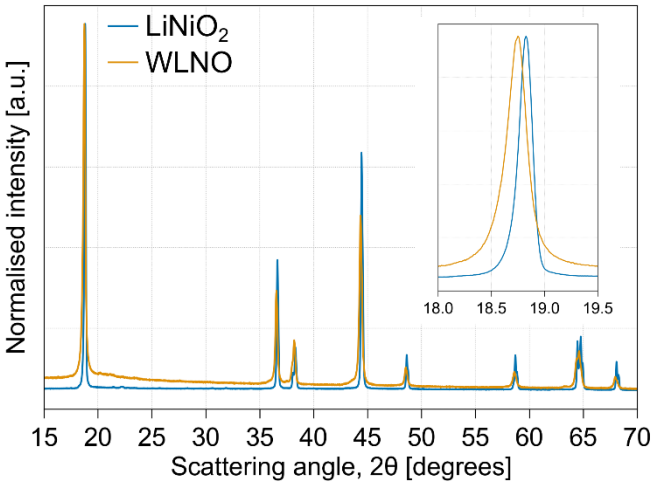

Figure S1: XRD data of undoped $LiNiO_2$ and WLNO, with their intensities normalised. The 003 reflection is highlighted in the inset.

1.3 Rietveld refinements

Rietveld refinements were performed in two stages: (1) to confirm the off-stoichiometry and (2) to evaluate the degree of Ni present in the Li layer. In each case, separate refinements were carried out with and without W in the structure, as the extent of W doping in the bulk was unclear. In general, the refinements were performed using the same methodology (background and peak shape parameters) as in the Pawley refinements. A structure model corresponding to $LiNiO_2$ was used for the refinement, with Ni and Li fully occupying the 3*a* and 3*b* sites, respectively. In the refinements with W, it was included in the 3*a* site leading to it having a distribution of 98% Ni and 2% W.

The off-stoichiometry was evaluated using the methodology presented in Ref.[11]. Here, all the site occupancies were fixed as per the stoichiometry and unit occupancy. The atomic displacement parameters (except that of W) were allowed to refine.

Table S2: Off-stoichiometry – Refined structural parameters using $LiNiO_2$ structure without W.

R_{wp}	GoF
6.56	4.05

a (b) (Å)	c (Å)	Vol. (Å^3)	Space group
2.88366(6)	14.2070(7)	102.312(7)	$R\bar{3}m$

Atom (site)	x/a	y/b	z/c	Occupancy	B_{iso} (Å^2)
Li (3*b*)	0	0	0.5	1	−3.95(15)
Ni (3*a*)	0	0	0	1	2.61(5)
O (6*c*)	0	0	0.2608(2)	1	2.79(7)

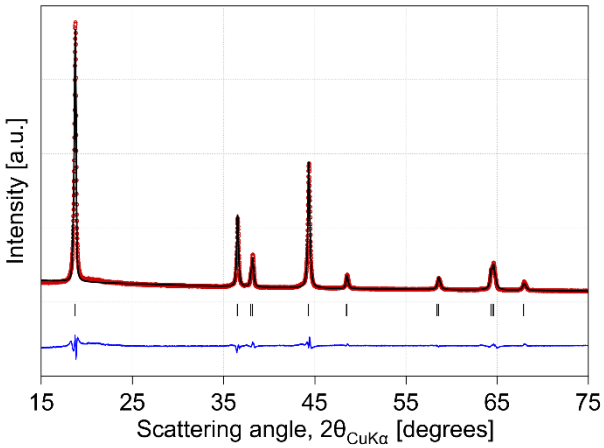

Figure S2: Refinement plot corresponding to the structure model presented in Table S2. The observed and calculated intensities are shown as red circles and black lines, respectively. The difference curve is shown in navy blue and the positions of the Bragg reflections as vertical tick markers.

Table S3: Off-stoichiometry – Refined structural parameters using $LiNiO_2$ structure with W.

R_{wp}	GoF
6.59	4.06

a (b) (Å)	c (Å)	Vol. (Å^3)	Space group
2.88366(6)	14.2070(6)	102.312(7)	$R\bar{3}m$

Atom (site)	x/a	y/b	z/c	Occupancy	B_{iso} (Å^2)
Li (3*b*)	0	0	0.5	1	−4.09(15)
Ni (3*a*)	0	0	0	0.98	2.99(5)
W (3*a*)	0	0	0	0.02	0.3
O (6*c*)	0	0	0.2608(2)	1	2.23(7)

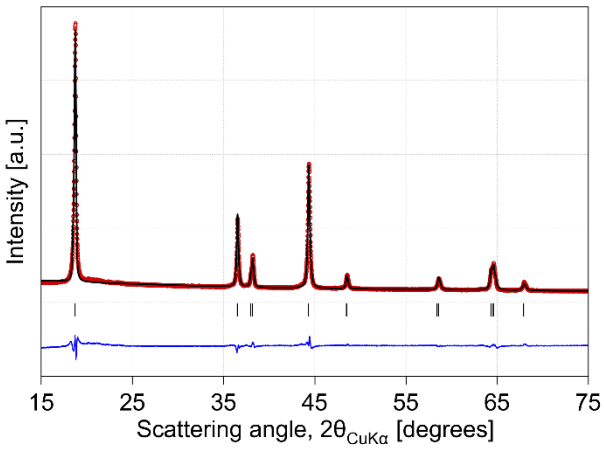

Figure S3: Refinement plot corresponding to the structure model presented in Table S3. The observed and calculated intensities are shown as red circles and black lines, respectively. The difference curve is shown in navy blue and the positions of the Bragg reflections as vertical tick markers.

Ni in the Li site (3*b*) was evaluated by refining the occupancy of that site, which was constrained to be 1. The isotropic atomic displacement parameters of Ni were constrained to be the same, and fixed to values obtained from Ref.[11].

Table S4: Li-Ni mixing – Refined structural parameters using $LiNiO_2$ structure <u>without</u> W.

R_{wp}	GoF
8.5	5.23

a (b) (Å)	c (Å)	Vol. (Å^3)	Space group
2.88367(6)	14.2067(7)	102.310(8)	$R\bar{3}m$

Atom (site)	x/a	y/b	z/c	Occupancy	B_{iso} (Å^2)
Li (3*b*)	0	0	0.5	0.977(2)	1.2
Ni (3*b*)	0	0	0.5	0.023(2)	0.5
Ni (3*a*)	0	0	0	1	0.5
O (6*c*)	0	0	0.2655(2)	1	0.8

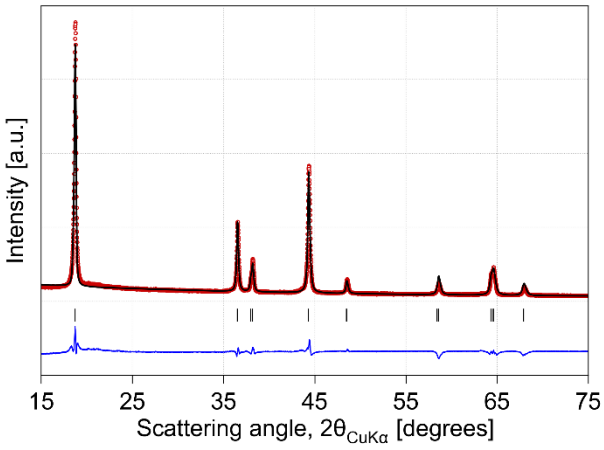

Figure S4: Refinement plot corresponding to the structure model presented in Table S4. The observed and calculated intensities are shown as red circles and black lines, respectively. The difference curve is shown in navy blue and the positions of the Bragg reflections as vertical tick markers.

Table S5: Li-Ni mixing – Refined structural parameters using $LiNiO_2$ structure with W.

R_{wp}	GoF
8.77	5.41

a (b) (Å)	c (Å)	Vol. (Å^3)	Space group
2.88365(8)	14.2070(9)	102.311(9)	$R\bar{3}m$

Atom (site)	x/a	y/b	z/c	Occupancy	B_{iso} (Å^2)
Li (3*b*)	0	0	0.5	0.979(2)	1.2
Ni (3*b*)	0	0	0.5	0.020(2)	0.5
Ni (3*a*)	0	0	0	0.98	0.5
W (3*a*)	0	0	0	0.02	0.5
O (6*c*)	0	0	0.2653(2)	1	0.8

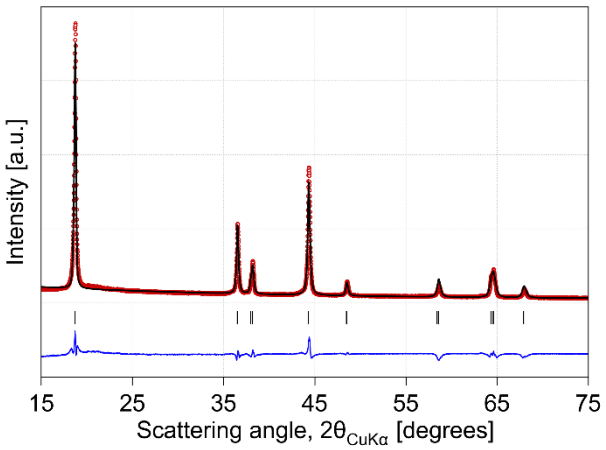

Figure S5: Refinement plot corresponding to the structure model presented in Table S5. The observed and calculated intensities are shown as red circles and black lines, respectively. The difference curve is shown in navy blue and the positions of the Bragg reflections as vertical tick markers.

2. XAS data of WLNO

2.1 Ni K-edge XANES data of pristine WLNO

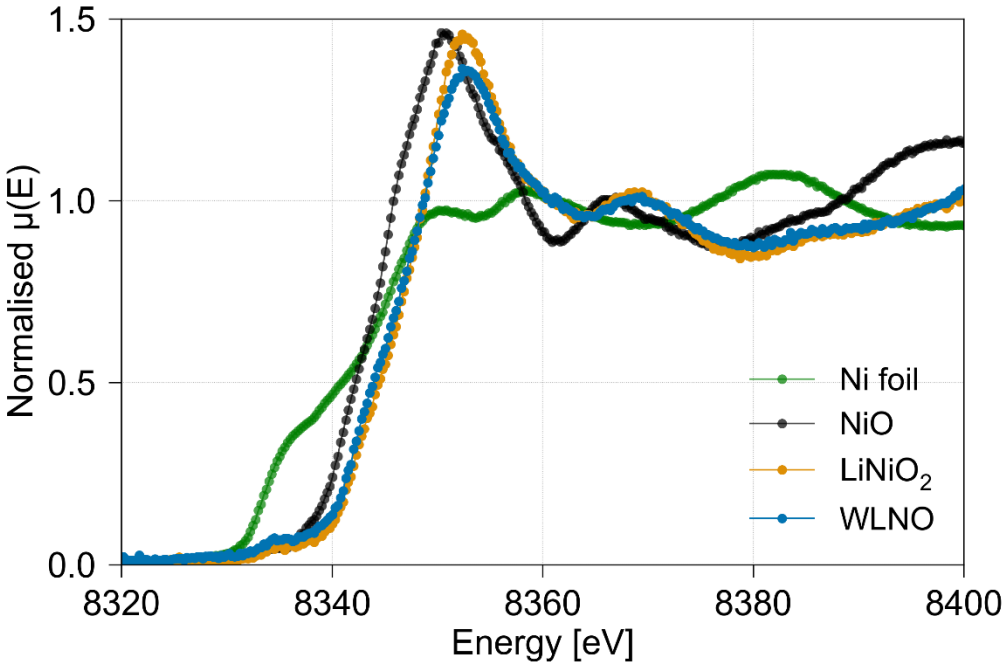

Figure S6: XANES spectra of WLNO with metallic Ni foil, NiO and $LiNiO_2$ for comparison.

2.2 Soft X-ray absorption spectra of WLNO electrode (OCV)

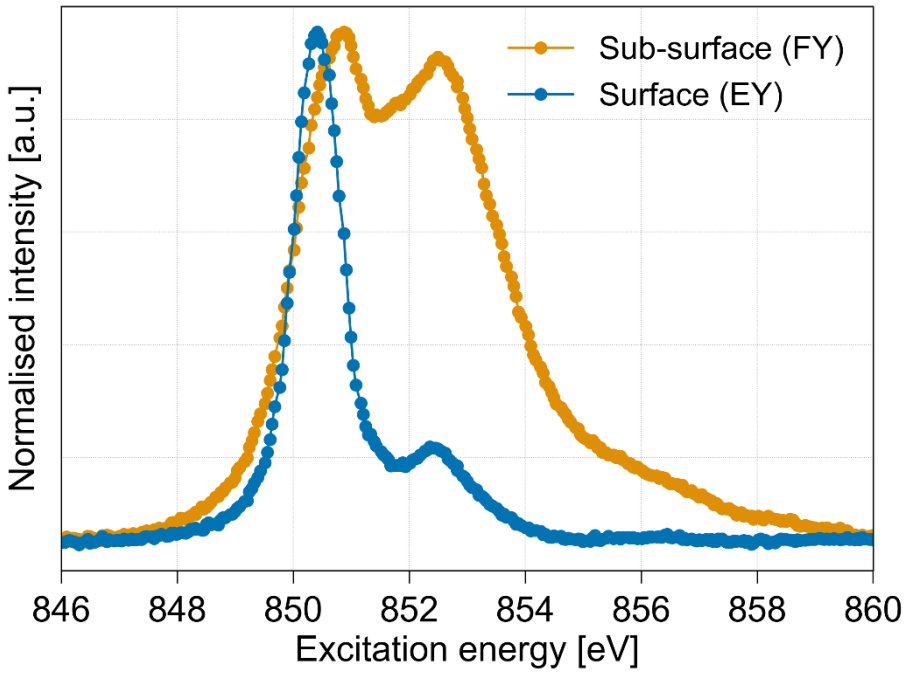

Figure S7: Soft X-ray absorption spectra of the WLNO electrode in the OCV state. FY and EY stands for fluorescence and electron yield, respectively

3. Pawley analysis of *ex situ* XRD data of cycled electrodes

Pawley analysis of the rhombohedral ($R\bar{3}m$) unit cell was performed using the same methodology as described in SI section 2.1. The specimen displacement (height error) due to the Al current collector was found out by refining it with the Al 220 peak (~65°), assuming the lattice parameter of Al to be 4.0495 Å ($Fm\bar{3}m$). The specimen displacement so obtained was held constant during the refinement of the WLNO $R\bar{3}m$ unit cell. In case of the discharged sample (Dch. 3V), the Al peak was not as strong as the rest of the samples, and so, slight variations in the specimen displacement, lattice parameters and unit cell volume values are expected. The graphite peak at ~26° was excluded in the refinement. The amorphous background due to the Kapton film was fit by linear interpolation of manually selected background points.

Table S6: Refined lattice parameters of $R\bar{3}m$ unit cell obtained after Pawley analysis of the ex situ WLNO electrodes XRD data

Sample	R_{wp}	GoF	a (b) (Å)	c (Å)	Vol. (Å^3)
OCV	7.46	5.45	2.88193(8)	14.1729(8)	101.943(8)
3.8 V	6.93	5.41	2.86390(1)	14.2684(9)	101.350(3)
4.2 V	7.24	5.42	2.83457(2)	14.338(1)	99.771(9)
4.5 V	8.25	6.33	2.8310(1)	14.257(2)	98.96(1)
4.7 V	8.84	7.07	2.8310(1)	14.229(2)	98.76(1)
Dch. 3 V	8.13	6.48	2.88090(7)	14.1889(5)	101.985(6)

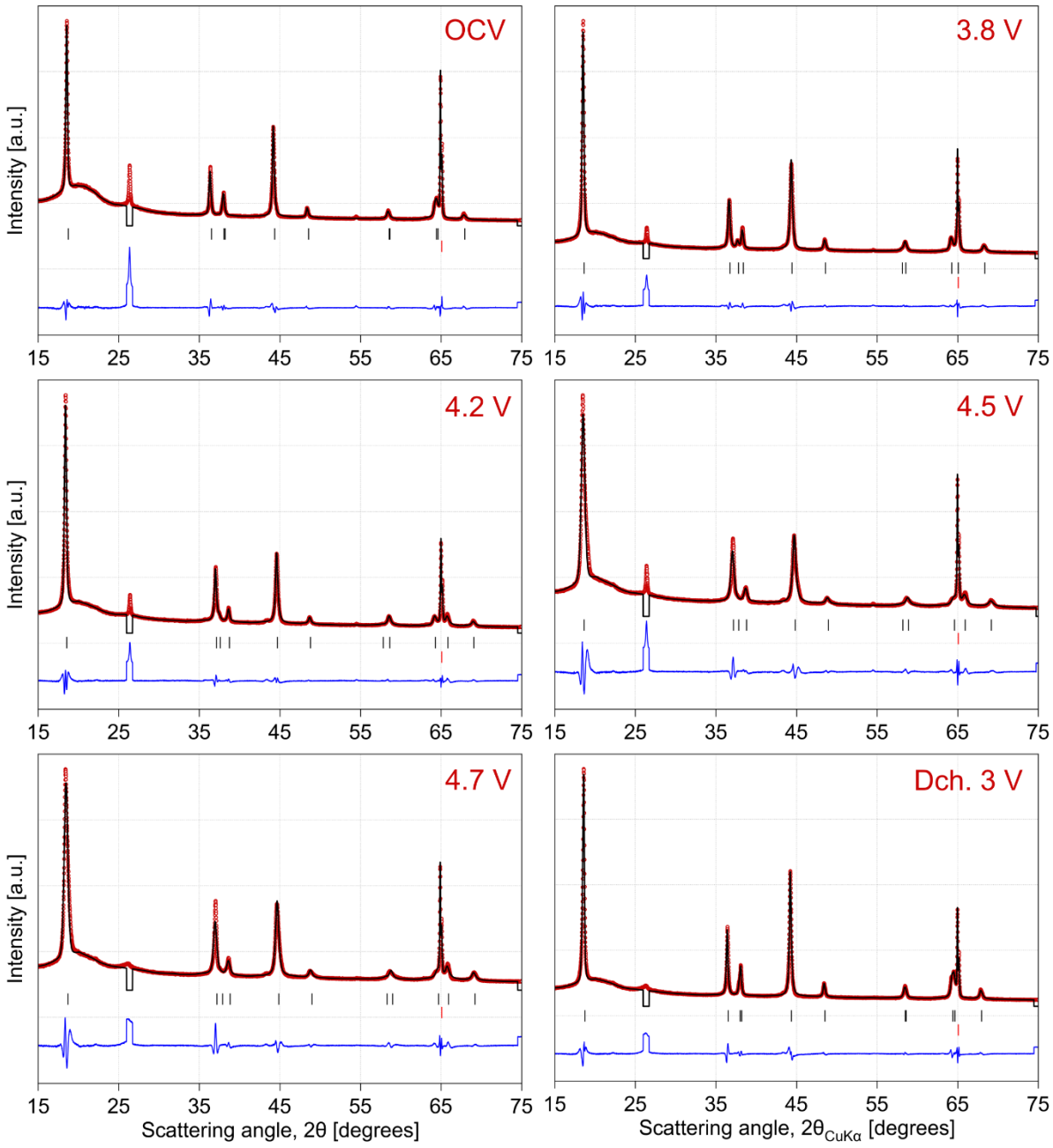

Figure S8: Pawley refinement plots of WLNO XRD data from electrodes. The observed and calculated intensities are shown as red circles and black lines, respectively. The difference curve is shown in navy blue and the positions of the Bragg reflections as vertical tick markers.

4. Soft XAS data of WLNO electrodes

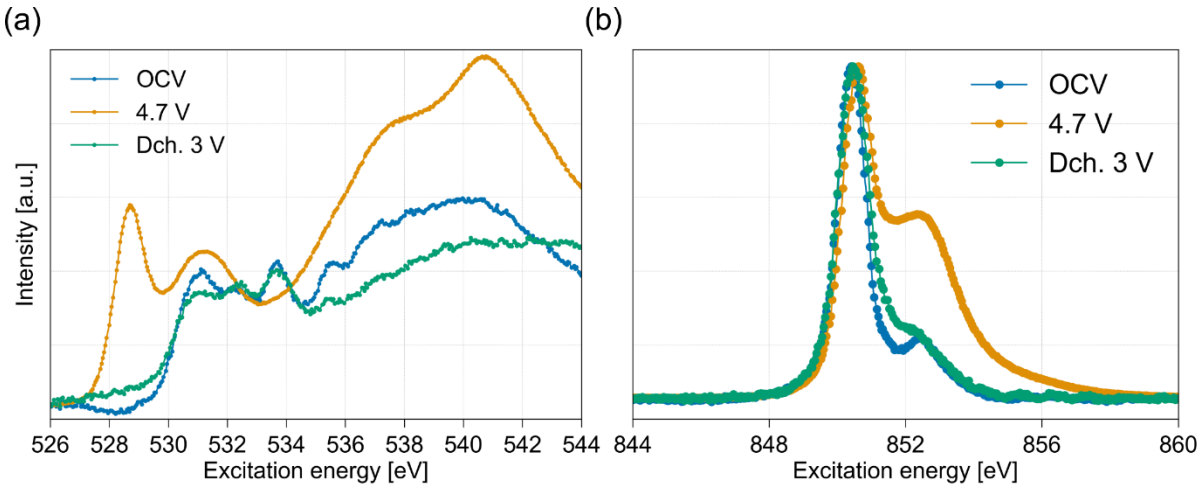

Figure S9: (a) O K-edge and (b) Ni L_3-edge spectra of WLNO collected in EY mode.

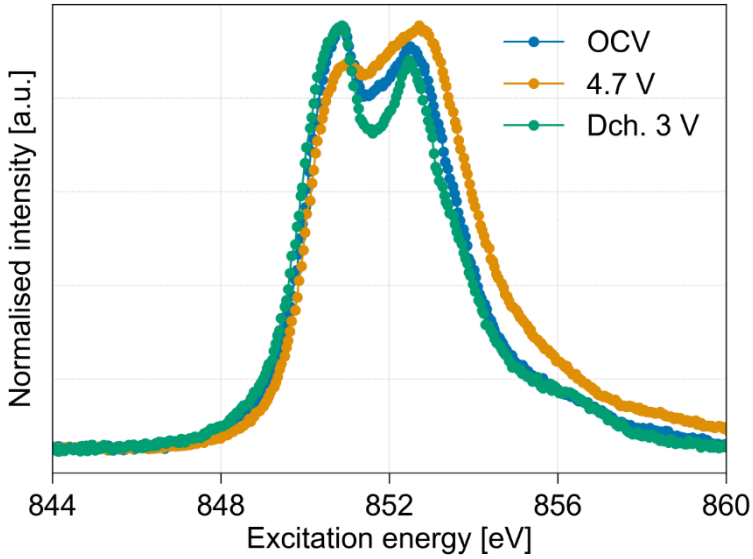

Figure S10: Ni L_3-edge spectra of WLNO collected in FY mode.

5. HAXPES data

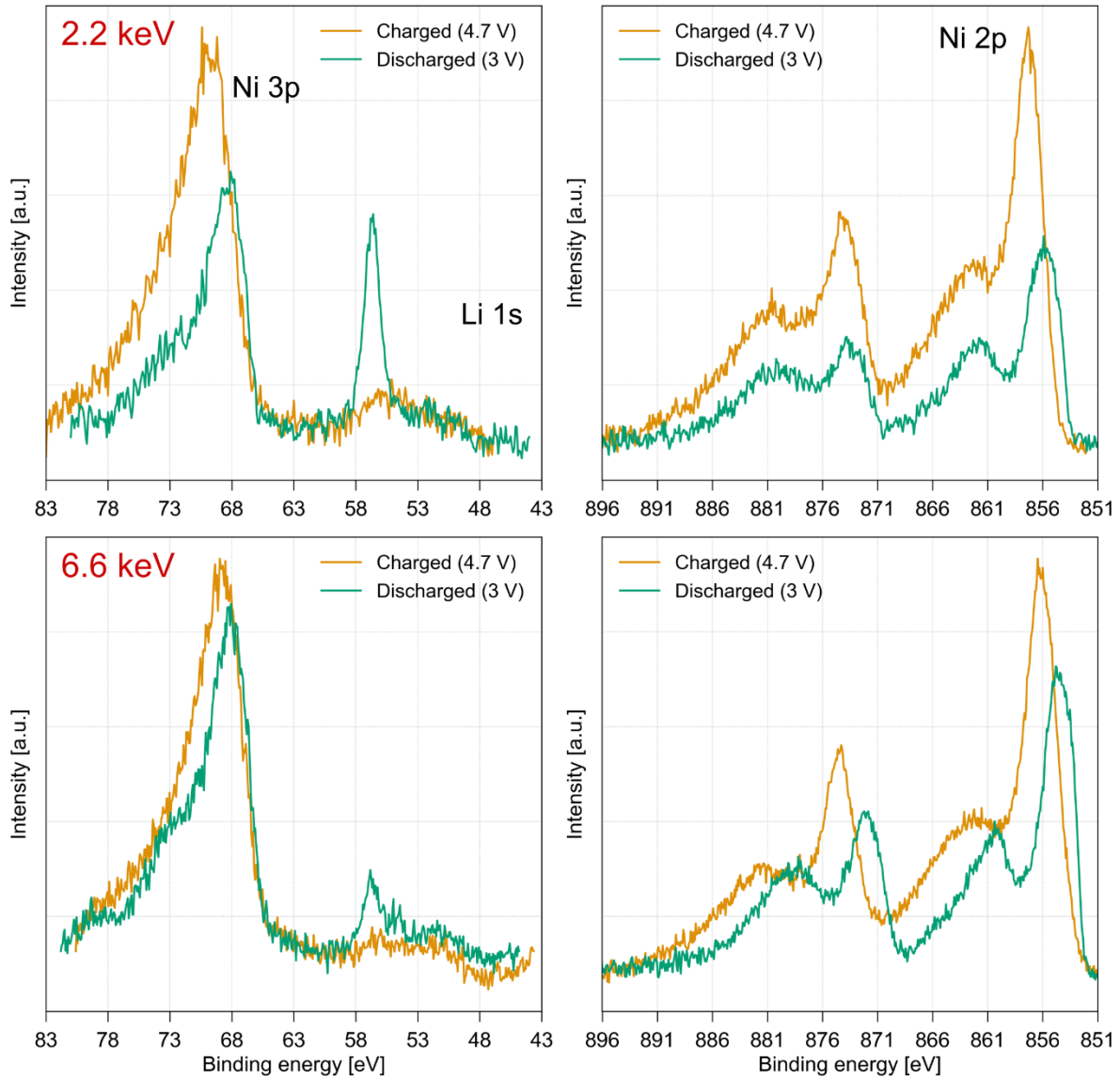

Figure S11: HAXPES data from the Li 1s and Ni 2p regions. The incident X-ray energy is shown in dark red. The OCV data is not included due to high noise levels caused by the surface organic species.

6. High resolution RIXS data

6.1 hr-RIXS maps

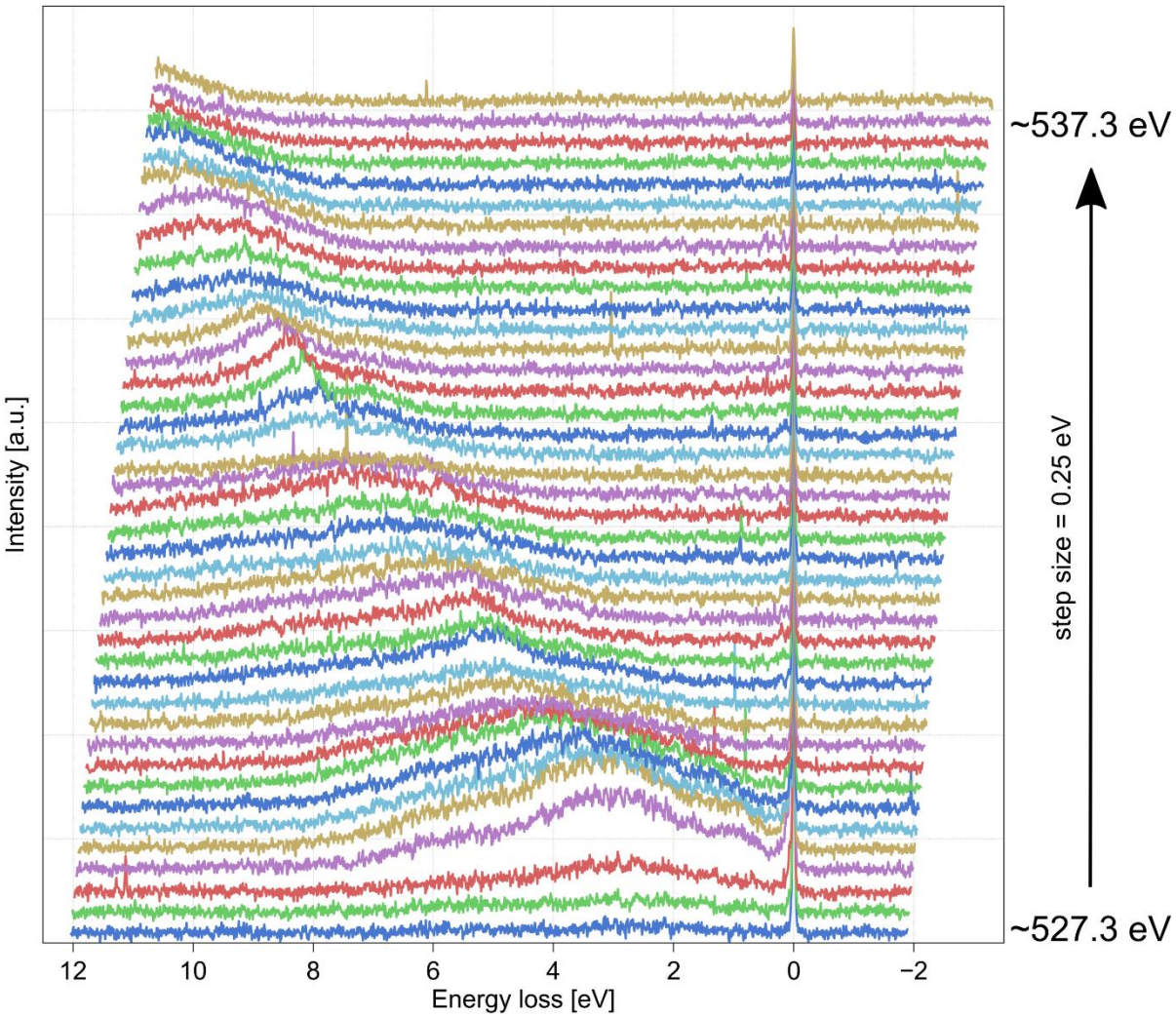

Figure S12: RIXS map for WLNO electrode in OCV state. The incident X-ray energy ranges from ~527 to ~537 eV, with a step size of 0.25 eV.

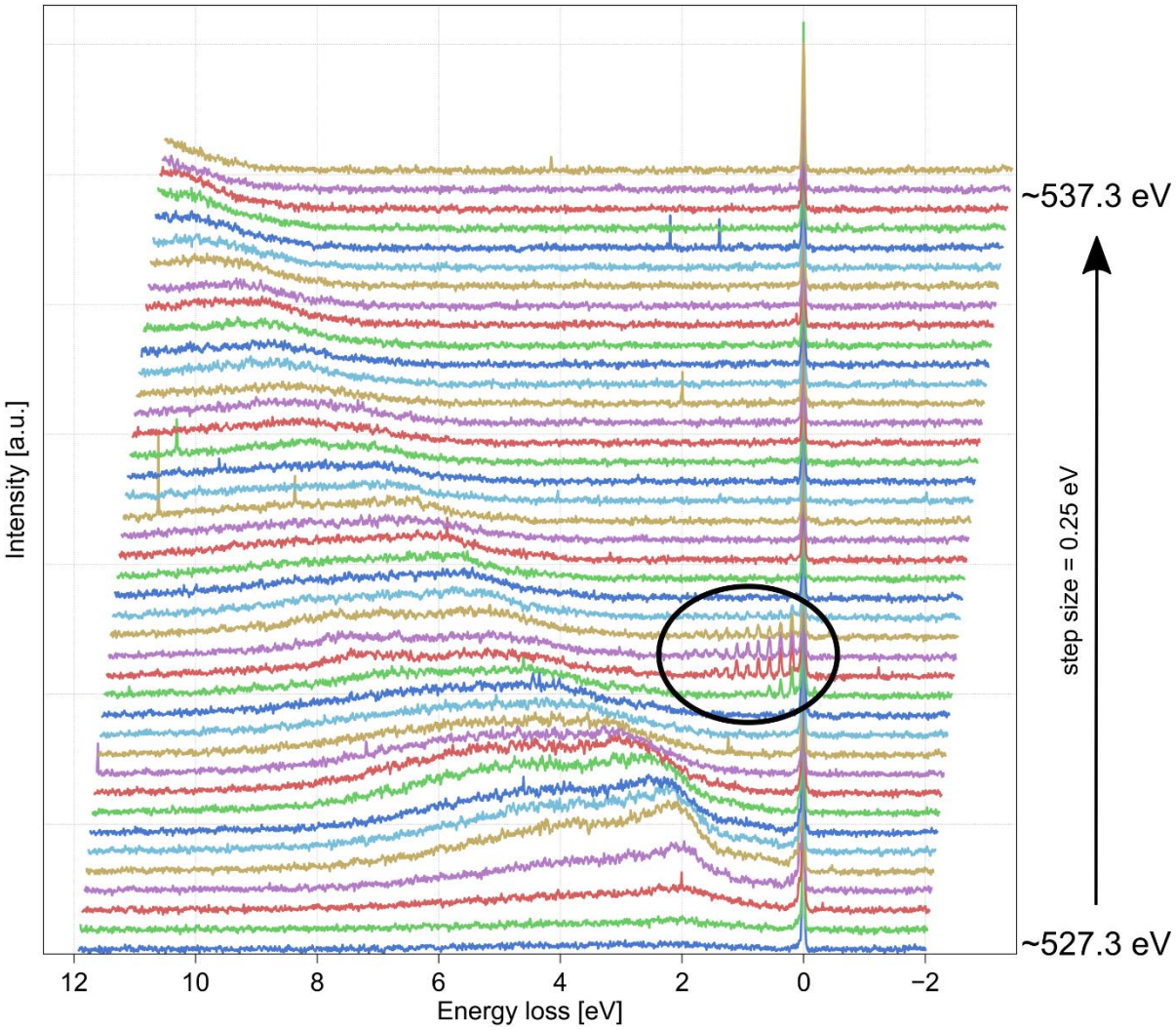

Figure S13: RIXS map for WLNO electrode charged to 4.7 V. The hr-RIXS feature is highlighted.

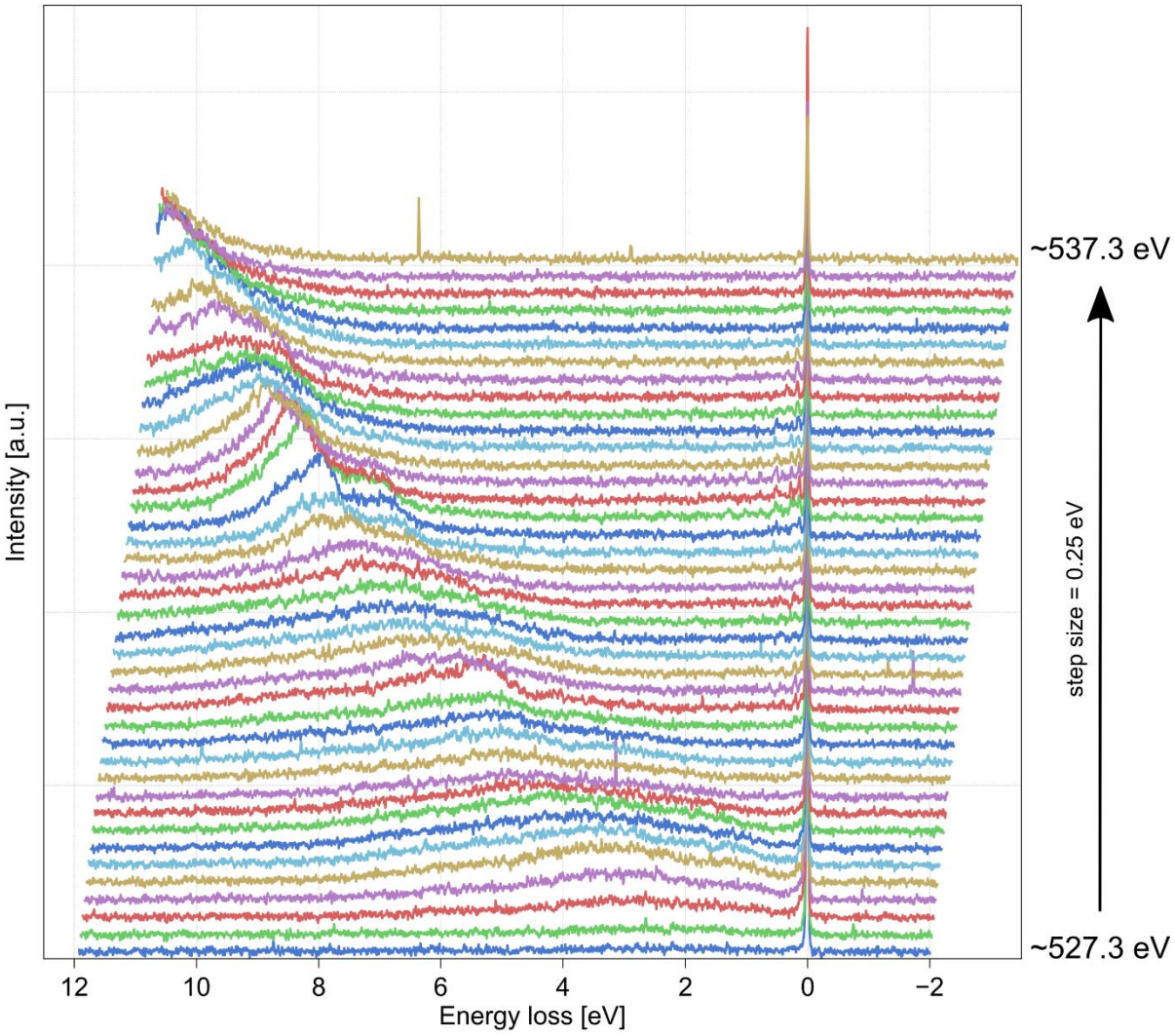

Figure S14: RIXS map for WLNO electrode discharged to 3V.

6.2 hr-RIXS line scans at ~531 eV

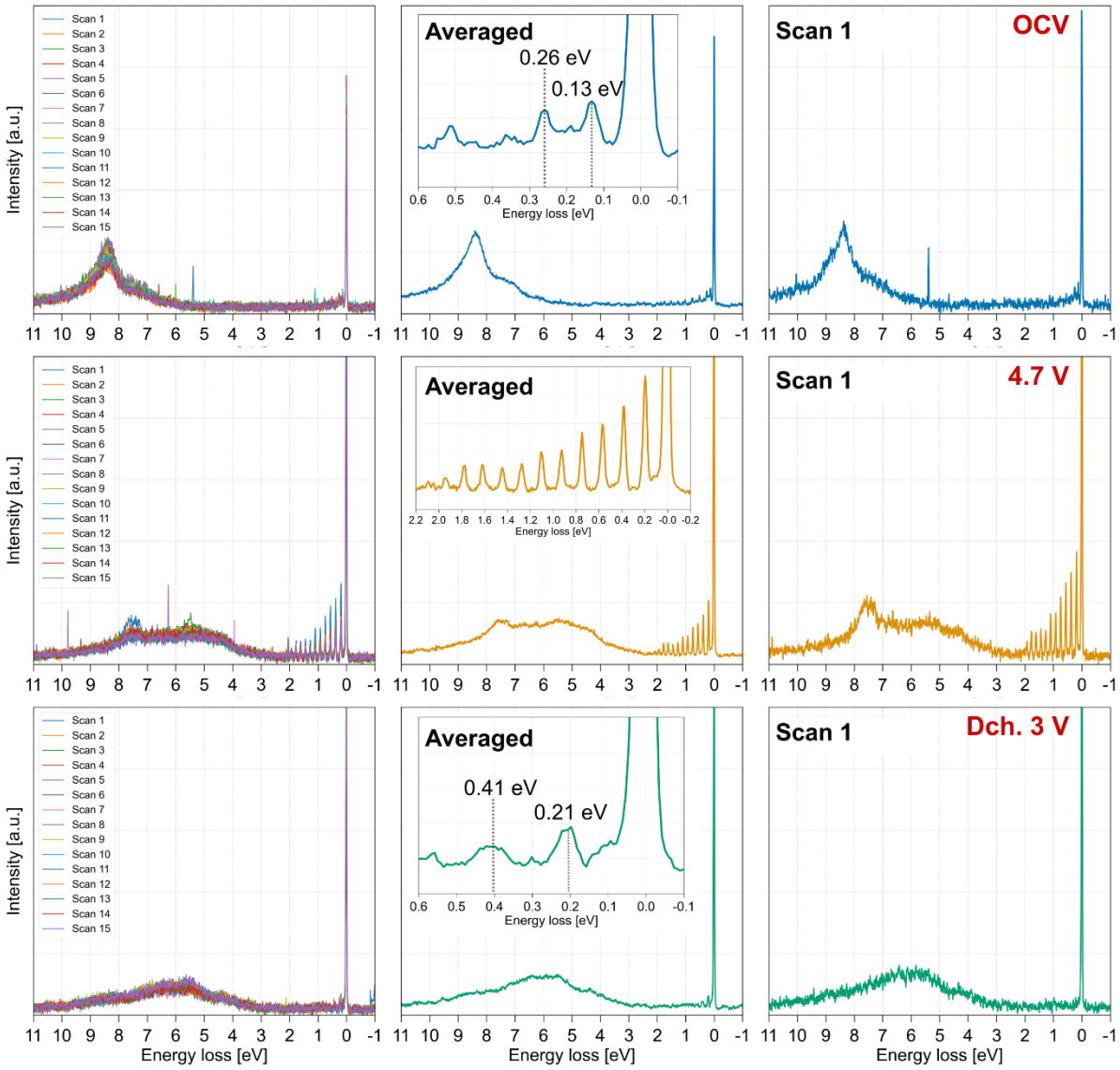

Figure S15: (Left) All 15 line scans collected on the three WLNO electrodes. (Centre) The averaged RIXS spectra of the 15 scans. (Right) The first RIXS line scan of each electrode. The sample names are shown in red on the top-right corner of the right panel.

References

[1] G. S. Pawley, Unit-Cell Refinement from Powder Diffraction Scans, Journal of Applied Crystallography **14**, 357 (1981).
[2] H. M. Rietveld, Line Profiles of Neutron Powder-Diffraction Peaks for Structure Refinement, Acta Crystallographica **22**, 151 (1967).
[3] H. M. Rietveld, A Profile Refinement Method for Nuclear and Magnetic Structures, Journal of Applied Crystallography **2**, 65 (1969).
[4] A. A. Coelho, Topasandtopas-Academic: An Optimization Program Integrating Computer Algebra and Crystallographic Objects Written in C++, Journal of Applied Crystallography **51**, 210 (2018).
[5] E. P. Jahrman, W. M. Holden, A. S. Ditter, D. R. Mortensen, G. T. Seidler, T. T. Fister, S. A. Kozimor, L. F. J. Piper, J. Rana, N. C. Hyatt, and M. C. Stennett, An Improved Laboratory-Based X-Ray Absorption Fine Structure and X-Ray Emission Spectrometer for Analytical Applications in Materials Chemistry Research, Review of Scientific Instruments **90**, 024106 (2019).
[6] B. Ravel and M. Newville, Athena, Artemis, Hephaestus: Data Analysis for X-Ray Absorption Spectroscopy Using Ifeffit, Journal of Synchrotron Radiation **12**, 537 (2005).
[7] K.-J. Zhou, A. Walters, M. Garcia-Fernandez, T. Rice, M. Hand, A. Nag, J. Li, S. Agrestini, P. Garland, H. Wang, S. Alcock, I. Nistea, B. Nutter, N. Rubies, G. Knap, M. Gaughran, F. Yuan, P. Chang, J. Emmins, and G. Howell, I21: An Advanced High-Resolution Resonant Inelastic X-Ray Scattering Beamline at Diamond Light Source, Journal of Synchrotron Radiation **29**, 563 (2022).
[8] M. Bianchini, A. Schiele, S. Schweidler, S. Sicolo, F. Fauth, E. Suard, S. Indris, A. Mazilkin, P. Nagel, S. Schuppler, M. Merz, P. Hartmann, T. Brezesinski, and J. Janek, From $LiNiO_2$ to Li_2NiO_3: Synthesis, Structures and Electrochemical Mechanisms in Li-Rich Nickel Oxides, Chemistry of Materials **32**, 9211 (2020).
[9] J. F. Mark Basham, Michael T. Wharmby, Peter C. Y. Chang, Baha El Kassaby, Matthew Gerring, Jun Aishima, Karl Levik, Bill C. A. Pulford, Irakli Sikharulidze, Duncan Sneddon, Matthew Webber, Sarnjeet S. Dhesi, Francesco Maccherozzi, Olof Svensson, Sandor Brockhauser, Gabor Naray and Alun W. Ashtona Data Analysis Workbench (Dawn), Journal of Synchrotron Radiation **22**, 853 (2015).
[10] H. Li, N. Zhang, J. Li, and J. R. Dahn, Updating the Structure and Electrochemistry of Li_xNiO_2 for $0 \leq x \leq 1$, Journal of The Electrochemical Society **165**, A2985 (2018).
[11] A. Rougier, P. Gravereau, and C. Delmas, Optimization of the Composition of the $Li_{1-z}Ni_{1+z}O_2$ Electrode Materials: Structural, Magnetic, and Electrochemical Studies, Journal of The Electrochemical Society **143**, 1168 (1996).